



Research article

Variants in the *ZNF469* gene in families with Brittle cornea syndrome and keratoconusQinghong Lin^{a,b,c,d,e,f,1}, Xuejun Wang^{a,b,c,d,e,1}, Tian Han^{a,b,c,d,e}, Xiaoliao Peng^{a,b,c,d,e}, Xingtao Zhou^{a,b,c,d,e,*}^a Department of Ophthalmology, Eye and ENT Hospital of Fudan University, Shanghai, 200000, China^b Eye Institute and Department of Ophthalmology, Eye & ENT Hospital, Fudan University, Shanghai, 200031, China^c NHC Key Laboratory of Myopia (Fudan University), Key Laboratory of Myopia, Chinese Academy of Medical Sciences, Shanghai, 200031, China^d Shanghai Research Center of Ophthalmology and Optometry, Shanghai, 200000, China^e Shanghai Engineering Research Center of Laser and Autostereoscopic 3D for Vision Care (20DZ2255000), Shanghai, 200000, China^f Refractive Surgery Department, Bright Eye Hospital, Shanghai, 200000, China

ARTICLE INFO

Keywords:

ZNF469

Brittle cornea syndrome

Keratoconus

ABSTRACT

Background: Brittle cornea syndrome 1 (BCS1) is a rare autosomal recessive disorder characterized by corneal and sclera thinning and fragility that is caused by zinc finger protein 469 (*ZNF469*) gene mutation. Keratoconus is another disease related to corneal thinning. Several reports have linked *ZNF469* variants and keratoconus. We recruited a four-generation BCS1 family and two keratoconus families to explore pathogenic *ZNF469* variants.

Methods: This study included 11 members from a family with BCS1, 2 families with keratoconus, 368 sporadic keratoconus patients and 325 unrelated healthy controls. Whole exome sequencing of DNA from peripheral blood and cross species conservation analysis was used to investigate and verify *ZNF469* variants.

Results: A new homozygous frameshift mutation c. 6727del (p.Asp2243Thr fs*8) in *ZNF469* was detected in the BCS1 family. Two *ZNF469* heterozygous variants g.88494671G > A (c.793G > A, p.G265S, rs754776767) were detected in keratoconus family 1 and a heterozygous missense variant g.88498262G > A (c.4384G > A, p.D1462 N, rs577890057) was found in keratoconus family 2. Based on the American College of Medical Genetics and Genomics guidelines, rs577890057 and rs754776767 were predicted to be variants of uncertain significance. c. 6727del (p. Asp2243Thr fs*8) in *ZNF469* was identified to be pathogenic.

Conclusions: We identified a new homozygous frameshift mutation and two heterozygous missense variations in *ZNF469* in the three families. Our findings extend the spectrum of *ZNF469* variants associated with keratoconus.

1. Introduction

Brittle cornea syndrome (BCS) is an autosomal recessive genetic disease characterized by an extremely thin cornea, progressive

* Corresponding author. Department of Ophthalmology, Eye and ENT Hospital of Fudan University, No. 83 Fenyang Road, Xuhui District, Shanghai, 200000, China.

E-mail address: Linqh19870624@163.com (X. Zhou).

¹ These authors contributed equally to this work and share first authorship.

spherical cornea or keratoconus (KC), high myopia, hearing loss and blue sclera. Patients with BCS have extremely fragile corneas, and even minor injuries can cause corneal rupture or perforation. BCS consists of two subtypes: BCS1 and BCS2. BCS1 is the result of mutation in the *ZNF469* gene, which encodes zinc finger protein 469 (ZNF469) [1–4].

Genome-wide association studies have identified central corneal thickness (CCT)-associated loci in healthy European and Asian populations [5,6]. CCT is associated with various diseases that may lead to blindness, such as KC. Single nucleotide polymorphism analysis of *ZNF469* has suggested that it is strongly associated with CCT, and recent studies have shown that common mutations in *ZNF469* influence CCT. Therefore, pathogenic *ZNF469* variants are not only pathogenic for BCS1, but these are also a potential risk factor for KC. KC is characterized by a gradual thinning and dilation of the cornea [7,8]. Both sporadic KC cases and KC families with variants in the *ZNF469* gene have been identified, which indicates a potential relationship between *ZNF469* and KC. *ZNF469* is therefore a candidate gene for the KC phenotype [9,10].

In this study, we recruited a four-generation family with BCS1 and two KC families and investigated the pathogenic variants of *ZNF469*. The relationship between the pathogenic variants of *ZNF469* and BC and KC was studied.

2. Materials and methods

2.1. Participants and examinations

We recruited 11 participants in this study including 5 members from a family with BCS1 and 6 members from 2 families with KC; this study also included 368 patients with sporadic KC and 325 unrelated healthy controls. Each participant underwent a comprehensive ocular examination including visual acuity, slit-lamp biomicroscopy, ophthalmoscopy, and cornea evaluations using a Scheimpflug camera system (Pentacam; Oculus Optikgeräte GmbH, Wetzlar, Germany), spherical equivalent diopter (ARK-530A, Nidek, Aichi, Japan) and fundus examination for both eyes. Color fundus photographs (CR-DG10, Canon, Tokyo, Japan) and optical coherence tomography (Heidelberg Spectralis OCT, Heidelberg Engineering GmbH, Germany) were also performed in most of the participants. This study was approved by the institutional review board of Fudan University (Shanghai, China) (approval no. 2022128) and performed in compliance with the Declaration of Helsinki. Written informed consent was obtained from all participants.

2.2. Whole exome sequencing and candidate variant screening

Whole exome sequencing of DNA from peripheral blood was performed in four members in the BCS1 family (IV:1, IV:2, III:1 and III:2) and all six members in the two KC families using a method described in our previous study [11]. Briefly, the whole exome was captured with SureSelect Human All Exon V6 kit (Agilent) and sequenced using the Illumina NovaSeq 6000 platform. Sequencing reads were obtained in the Fastq format. The reads were mapped to human genome GRCh37 using Burrows Wheeler Aligner (BWA). Variants were called using the Genome Analysis Toolkit (GATK), followed by variant annotation through ANNOVAR.

Variant discovery and genotyping were performed with GATK (<https://software.broadinstitute.org/gatk/>) and annotated with ANNOVAR. Common variants, such as intergenic, upstream, downstream, intronic, and synonymous variants, and variants with minor allele frequency (MAF) > 1% in the 1000 genome, ExAC, and gnomAD databases, were filtered out. In silico programs were used to predict the deleterious effect of each variant on the function of the proteins, including REVEL, ClinPred, SIFT, Polyphen2, LRT, Mutation Assessor, PROVEAN, CADD, MutationTaster, dbcsnv11_AdaBoost, dbcsnv11_RandomForest, and Human Splicing Finder (HSF). Genotype-phenotype analyses were performed using the Exomiser and Phenolyzer software programs. Finally, the results were read following the standards and guidelines of American College of Medical Genetics and Genomics (ACMG).

A segregation analysis was performed on these families. Only the mutations shared by members from two families with KC were considered as candidate mutations.

2.3. Variant validation and cross-species conservation analysis

All variants were analyzed by online software including Polyphen2 (genetics.bwh.harvard.edu), SIFT (sift.jcvi.org), FATHMM-MKL (<http://fathmm.biocompute.org.uk>), CADD v1.4 (cadd.gs.washington.edu), PROVEAN (jcv.org/research/provean), Mutation Taster (mutationtaster.org) and American College of Medical Genetics and Genomics (ACMG) guidelines. Polymerase chain reaction (PCR) and Sanger sequencing were conducted in other family members and controls to confirm each candidate variant. The PCR primers were designed using Primer3. The validation and analyses were conducted using NCBI VARIANT, NCBI HomoloGene and 1000 Genomes Project databases. Amino acid sequences of both the wild-type and the mutant ZNF469 from Mutalyzer (<https://mutalyzer.nl/>) were used to predict the three-dimensional (3D) protein structures of ZNF469 by I-TASSER.

2.4. Analysis of the protein-protein interaction (PPI) network

We used the STRING database and Cytoscape (v3.9.0) software to analyze the PPI network. Proteins more than or equal to 5° were set as crucial proteins in the PPI network.

2.5. Statistical analysis

For baseline characteristics of the study subjects, patients and controls were matched on gender (χ^2 test) and age (T-test).

Differences in age were adjusted with logistic regression.

The allele and genotype frequencies of the SNPs were compared between the patients and controls. We evaluated the frequency of the genotypes and alleles in this study using the χ^2 test. $p < 0.05$ was considered statistically significant.

3. Results

3.1. Clinical manifestations

The family trees of the three families included in this study are shown in Fig. 1a, b and 1c. Information on the family/proband and their characteristics are shown in Table 1. In the BCS1 family, there were two affected individuals (I:2 and IV:1). The proband of this family (IV:1) was a 38 years old male, and vision in the left eye was counting fingers. When the proband was four years old, he underwent enucleation because of a slight collision that resulted in corneal rupture in his right eye. The cornea in the left eye was extremely thin with keratoglobus, and the CCT was approximately 160 μm . The maximum value of keratometry for the left eye was 64.2 D (Fig. 2a). The axis length was 28.59 mm in the left eye. He had high myopia with chorioretinopathy, peripapillary atrophy and macular hemorrhage in the left eye (Fig. 2b). He also had skeletal system abnormalities such as joint hypermobility and flat feet (Fig. 2c and d).

III:1 had a CCT of 464 μm in the right eye and 471 μm in the left eye (Fig. 2e). The CCT of both eyes of III:2 was 510 μm (Fig. 2f). I:2 also underwent enucleation in the left eye because of corneal rupture after trauma while taking care of a child.

In KC family 1, two members were diagnosed with KC. The proband (II.1) was a 17-year-old male. The visual acuity in both eyes was 10/50. The corrected distance visual acuity in the right eye with $-2.00\text{DS}/-1.50\text{DC} \times 90^\circ$ was 20/20 and in the left eye with $-2.50\text{DS}/-2.50\text{DC} \times 120^\circ$ was 30/50. The maximum anterior surface curvature (MASC) was 50.0 D in the right eye and 52.7 D in the left eye. The means of posterior elevation of the cornea (PEC) were 23 μm in the right eye and 49 μm in the left eye; the CCT was 475 μm in the right eye and 463 μm in the left eye (Fig. 3a). Belin analysis for patient II.1 showed that the corneal thickness progression deviation (Dp) value was 5.47 in the right eye and 8.81 in the left eye. The Pentacam tomographic composite index (BAD-D) of both eyes demonstrated a marked pathological change (5.42 in the right eye and 7.56 in the left eye) (Fig. 3b).

The mother of the proband (I.1) was 37 years old; the CCT was 464 μm in the right eye and 471 μm in the left eye (Fig. 3c), and Belin analysis showed that the BAD-D in the right eye was suspected for KC (1.70, Fig. 3d).

The proband (II.1) of KC family 2 was a 22-year-old male. His presenting visual acuity was 10/50 in the right eye and 20/20 in the left eye. The corrected distance visual acuity in the right eye with $-3.50\text{DS}/-3.50\text{DC} \times 150^\circ$ was 20/50 and in the left eye with -0.50DS was 20/20. The means of PEC were 40 μm in the right eye and 8 μm in the left eye. The MASC was 53.1 D in the right eye and 45.1 D in the left eye. The CCT of the right eye was 468 μm and 485 μm in the left eye (Fig. 4a). Belin analysis of the proband showed that both Dp values were in a suspicious state (6.28 in the right eye and 2.25 in the left eye). The BAD-D demonstrated a marked pathological change in the right eye (6.80 and 2.78 in the right and left eye, respectively) (Fig. 4b).

The mother of the proband (I.1) was 44 years old. Her presenting visual acuity was 40/50 and corrected distance visual acuity was 20/20 in both eyes, with $-1.00\text{DS}/-1.00\text{DC} \times 180^\circ$ correction in the right eye and $-1.50\text{DS}/-1.50\text{DC} \times 150^\circ$ correction in the left eye. The MASC was 46.4 D (right eye) and 48.4 D (left eye). The PEC value at the thinnest point of the cornea was within the normal

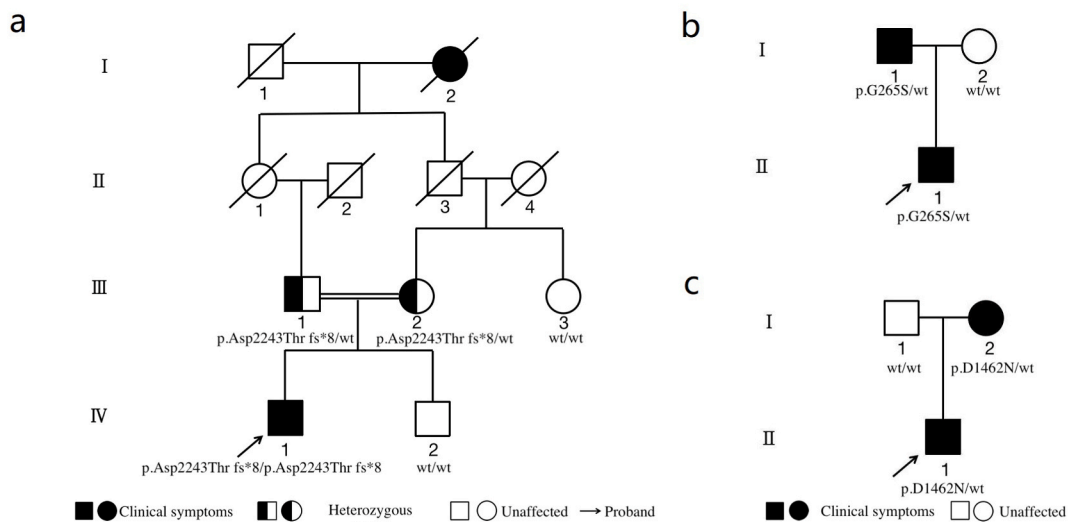


Fig. 1. The family trees of the three families included in this study. **a:** A four-generation Chinese BCS1 family; **b:** The keratoconus family 1 with two keratoconus patients; **c:** The keratoconus family 2 with two keratoconus patients. The square indicates male patients and the circle indicates female patients. The solid symbol indicates the affected individual, while the open symbol indicates an unaffected family member. The diagonal line indicates that a family member has passed away. The proband is indicated by an arrow.

Table 1
Characteristics of the family members in this study.

Family member	Gender/Age	CCT (μm)	Kmax (D)	PEC (μm)	Surgery	Eye disease	Genetic finding
BCS1 Family							
IV:1	M/38	160 (OS) NA (OD)	64.2 (OS) NA (OD)	21 (OS) NA (OD)	Enucleation (OD)	keratoglobus	homozygous frameshift mutation c. ZNF469; 6727del (p. Asp2243Thr fs*8)
IV:2	M/35	523 (OD) 518 (OS)	45.9 (OD) 45.3 (OS)	5 (OD) 3 (OS)	–	–	–
III:1	M/62	464 (OD) 471 (OS)	47.2 (OD) 46.6 (OS)	9 (OD) 7 (OS)	–	–	heterozygous frameshift; ZNF469; 6727del (p. Asp2243Thr fs*8)
III:2	F/58	510 (OD) 510 (OS)	45.6 (OD) 45.5 (OS)	4 (OD) 3 (OS)	–	–	heterozygous frameshift; ZNF469; 6727del (p. Asp2243Thr fs*8)
III:3	F/49	553 (OD) 547 (OS)	47.6 (OD) 47.3 (OS)	11 (OD) 8 (OS)	–	–	–
II:1	F/Passed away	NA	NA	NA	NA	NA	NA
II:2	M/Passed away	NA	NA	NA	NA	NA	NA
II:3	M/Passed away	NA	NA	NA	NA	NA	NA
II:4	F/Passed away	NA	NA	NA	NA	NA	NA
I:1	M/Passed away	NA	NA	NA	NA	NA	NA
I:2	F/Passed away	NA	NA	NA	Enucleation (OS)	keratoglobus	NA
KC Family1							
II:1	M/17	475 (OD) 463 (OS)	50.0 (OD) 52.7 (OS)	23 (OD) 49 (OD)	–	keratoconus	heterozygous variants g.88494671G > A (c.793G > A, p. G265S, rs754776767)
I:1	M/37	474 (OD) 472 (OS)	44.1 (OD) 44.3 (OS)	4 (OD) 4 (OS)	–	keratoconus	heterozygous variants g.88494671G > A (c.793G > A, p. G265S, rs754776767)
I:2	F/40	545 (OD) 542 (OS)	42.8 (OD) 44.9 (OS)	3 (OD) 4 (OS)	–	–	–
KC Family2							
II:1	M/22	468 (OD) 485 (OS)	53.1 (OD) 45.1 (OS)	40 (OD) 8 (OD)	–	keratoconus	heterozygous missense mutation g.88498262G > A (c.4384G > A, p.D1462 N, rs577890057)
I:1	M/46	563 (OD) 558 (OS)	47.5 (OD) 47.5 (OS)	6 (OD) 9 (OS)	–	–	–
I:2	F/44	449 (OD) 435 (OS)	46.4 (OD) 48.4 (OS)	14 (OD) 30 (OS)	–	keratoconus	heterozygous missense mutation g.88498262G > A (c.4384G > A, p.D1462 N, rs577890057)

M: male, F: Female, OD: right eye; OS: left eye; CCT: central corneal thickness; NA: not available.

range in both eyes (14 and 30 μm in the right and left eye, respectively). She also exhibited central cornea thinning, and the CCT was 449 μm in the right eye and 435 μm in the left eye (Fig. 4c). Belin analysis showed that BAD-D value was in a suspicious state (2.00 and 5.62 in the right and left eye, respectively) (Fig. 4d).

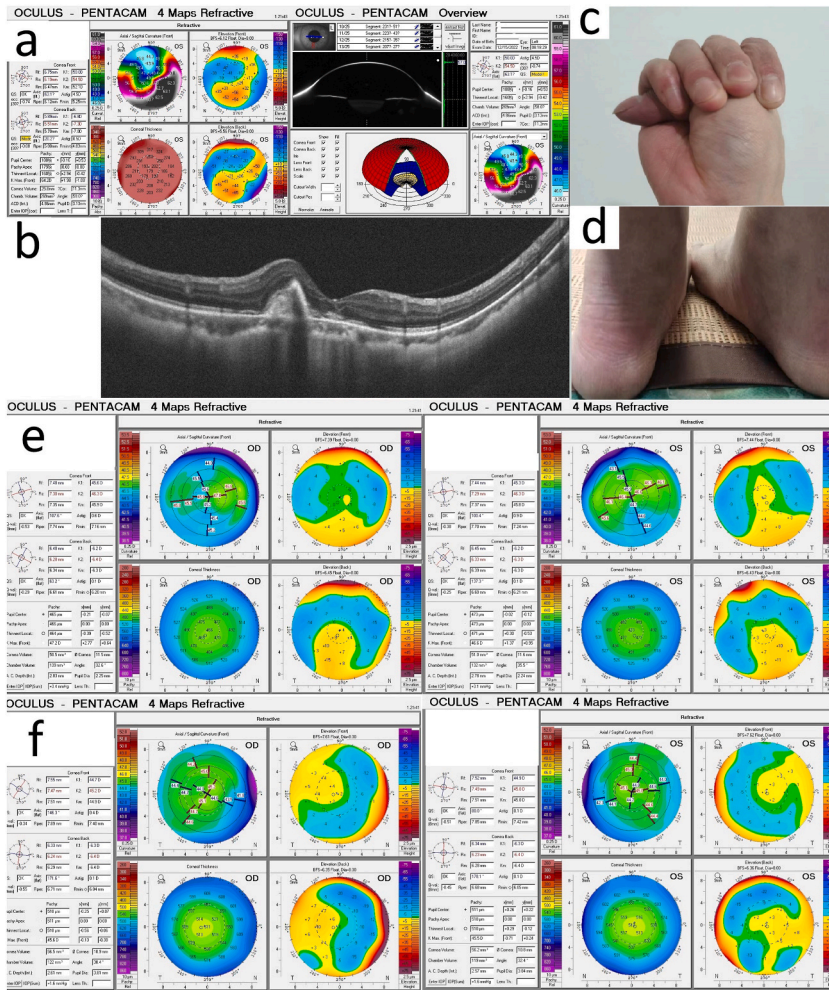


Fig. 2. Clinical manifestations of family members in the BCS1 family. **A:** The corneal topography (Pentacam) reports for proband IV.1 in the BCS1 family. The central corneal thickness was 160 μm . The maximum keratometry value was 64.2 in the left eye; **b:** Optical coherence tomography showed macular hemorrhage in the left eye; **c:** Joint hypermobility; **d:** Flat feet; **e:** III:1, the central corneal thickness was 464 μm in the right eye and 471 μm in the left eye; **f:** III:2, the central corneal thickness was 510 μm for both eyes.

3.2. Identification and analyses of a new variant in ZNF469

Whole exome sequencing results for these three pedigrees were analyzed, and candidate variants were screened (see [Supplementary Table 1](#) for the filtering criteria and the number of variants in each filtering process). The disease-related candidates in the BCS1 family are shown in the [Supplemental Table 2](#). A homozygous frameshift mutation c. 6727del (p.Asp2243Thr fs*8) in *ZNF469* with low frequency in general population that matched co-segregation in the BCS1 family was identified. This frameshift mutation occurred in the coding region and was a deletion of guanine at position 6727, which caused an amino acid change (aspartic acid changed to threonine) at residue 2243. After a frameshift of eight amino acids, an early termination codon was induced. III:1 and III:2 carried this heterozygous frameshift mutation, while IV:2 and III:3 did not ([Fig. 5a](#)).

We also found two *ZNF469* heterozygous variants in the two KC families ([Supplementary Table 2](#)). The proband in KC family 1 carried a heterozygous missense variant g.88494671G > A (c.793G > A, p.G265S, rs754776767), and the proband in KC family 1 carried a heterozygous missense variant g.88498262G > A (c.4384G > A, p.D1462N, rs577890057) ([Fig. 5b](#) and [c](#)). Both variants were absent in other healthy family members and controls. The detection rates of rs754776767, rs577890057 and c. 6727del (p. Asp2243Thr fs*8) in *ZNF469* were much higher in the 368 sporadic keratoconus patients compared with the healthy controls ([Tables 2–5](#)).

In online prediction programs [12], rs577890057 and rs754776767 were predicted to be variants of uncertain significance (VUS). c. 6727del (p. Asp2243Thr fs*8) in *ZNF469* was identified to be pathogenic ([Table 6](#)). The report for the cross-species conservation analysis indicated that the glycine at codon 265 and aspartic acid at codon 1462 of *ZNF469* are highly conserved ([Supplementary Fig. 1](#)). The 3D models of the wild-type protein and these two variants in [Fig. 6a](#) and [b](#) show the conformational changes caused by this

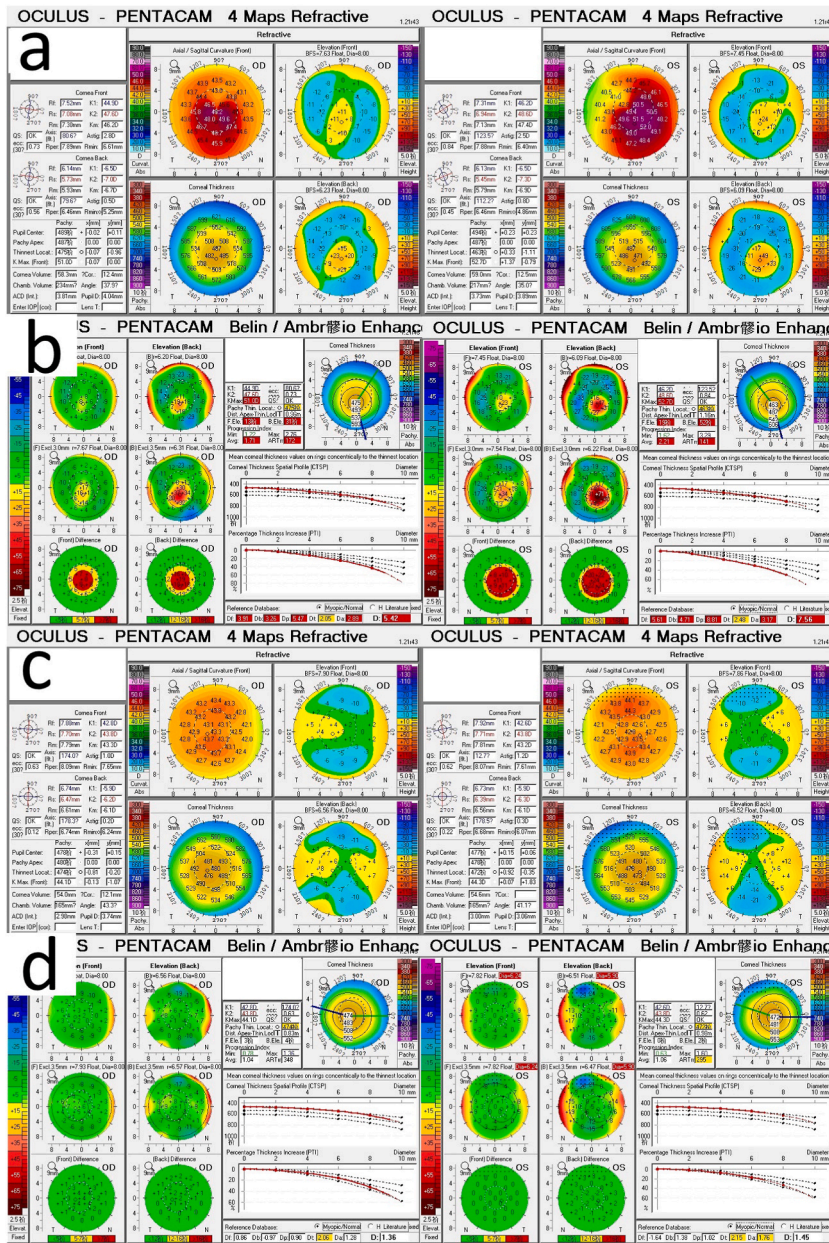


Fig. 3. Clinical manifestations of family members in KC family 1. **A:** The corneal topography (Pentacam) reports for proband II:1 in KC family 1. The means of posterior elevation of the cornea was 23 μm in the right eye and 49 μm in the left eye. The central corneal thickness was 475 μm in the right eye and 463 μm in the left eye; **b:** The Belin analysis for patient II.1 showed that the Dp value was 5.47 in the right eye and 8.81 in the left eye. The BAD-D of both eyes demonstrated a marked pathological change (5.42 in right eye and 7.56 in left eye); **c:** The central corneal thickness of I.1 was 464 μm in the right eye and 471 μm in the left eye; **d:** Belin analysis of I.1 showed that the BAD-D value in the right eye was in a suspicious state (1.70).

mutation.

3.3. Topological analysis of PPI networks

Eight significantly enriched genes were imported to STRING platform to construct a PPI network; it was then imported in Cytoscape to screen the core target genes. As shown in Fig. 7a and b, ZNF469 (with the high degree of 24) was set as a crucial protein and placed in the middle of the PPI network.

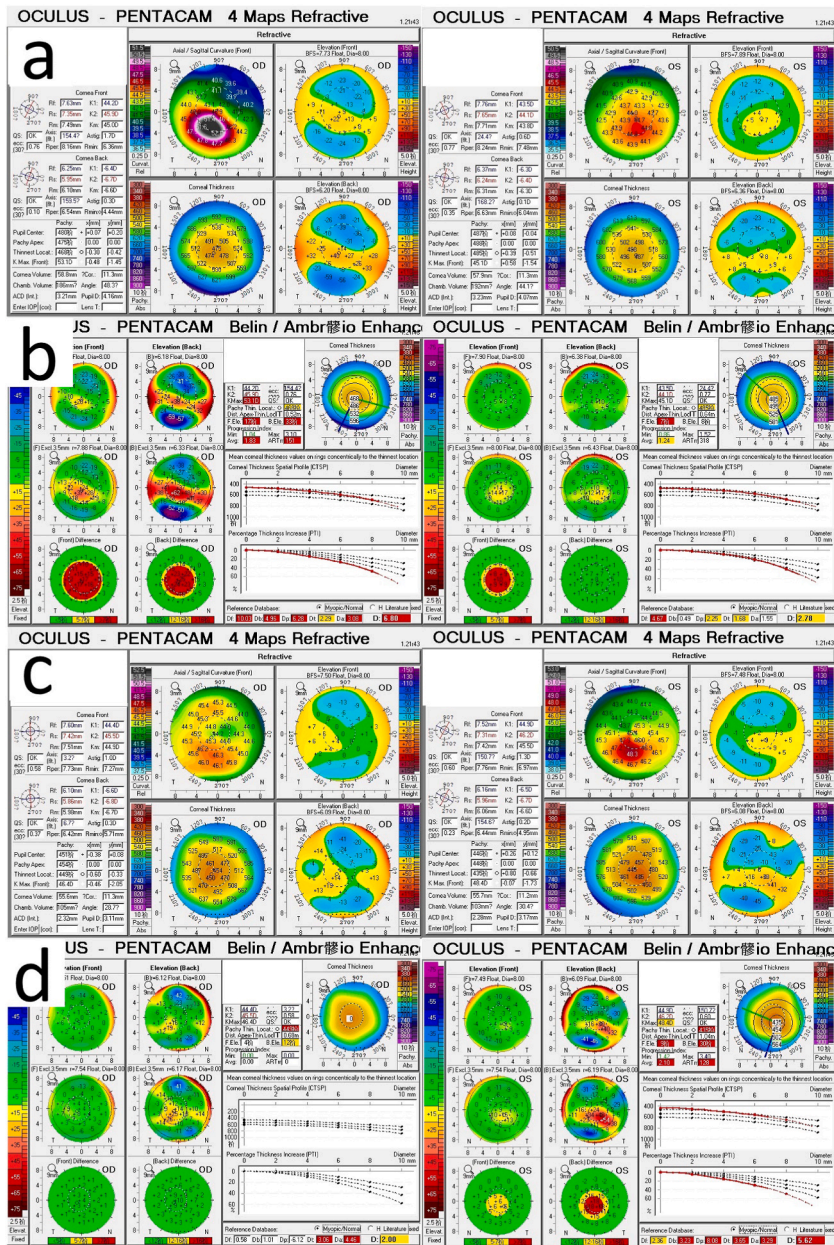


Fig. 4. Clinical manifestations of family members in KC family 2. **a:** The corneal topography (Pentacam) reports for proband II:1 in KC family 2. The means of posterior elevation of the cornea was 40 μm in the right eye and 8 μm in the left eye. The maximum anterior surface curvature was 53.1 D (right eye) and 45.1 D (left eye). The central corneal thickness was 468 μm (right eye) and 485 μm (left eye); **b:** Belin analysis of the proband (II.1) showed that both Dp values were in a suspicious state (6.28 and 2.25 in the right and left eyes, respectively). The BAD-D demonstrated a marked pathological change in the right eye (6.80); **c:** In I.1, the posterior elevation of the cornea values at the thinnest point of the cornea were within normal range in both eyes (14 and 30 μm in the right and left eyes, respectively). The central corneal thickness was 449 μm in the right eye and 435 μm in the left eye; **d:** Belin analysis of I.1 showed that BAD-D values were in a suspicious state (2.00 and 5.62 in the right and left eyes, respectively).

4. Discussion

In our study, we examined a four-generation consanguineous Chinese BCS1 family and two KC families. In the BCS1 family, two affected family members exhibited corneal rupture from a slight collision. We identified a novel homozygous frameshift mutation c. 6727del (p.Asp2243Thr fs*8) in the *ZNF469* gene, which was a deletion of guanines at position 6727 in the coding region that changed an aspartic acid to threonine at residue 2243. After a frameshift of eight amino acids, an early stop codon was induced; we speculate that this may lead to nonsense-mediated mRNA decay. According to the ACMG guidelines [12], the mutation is likely to be pathogenic;

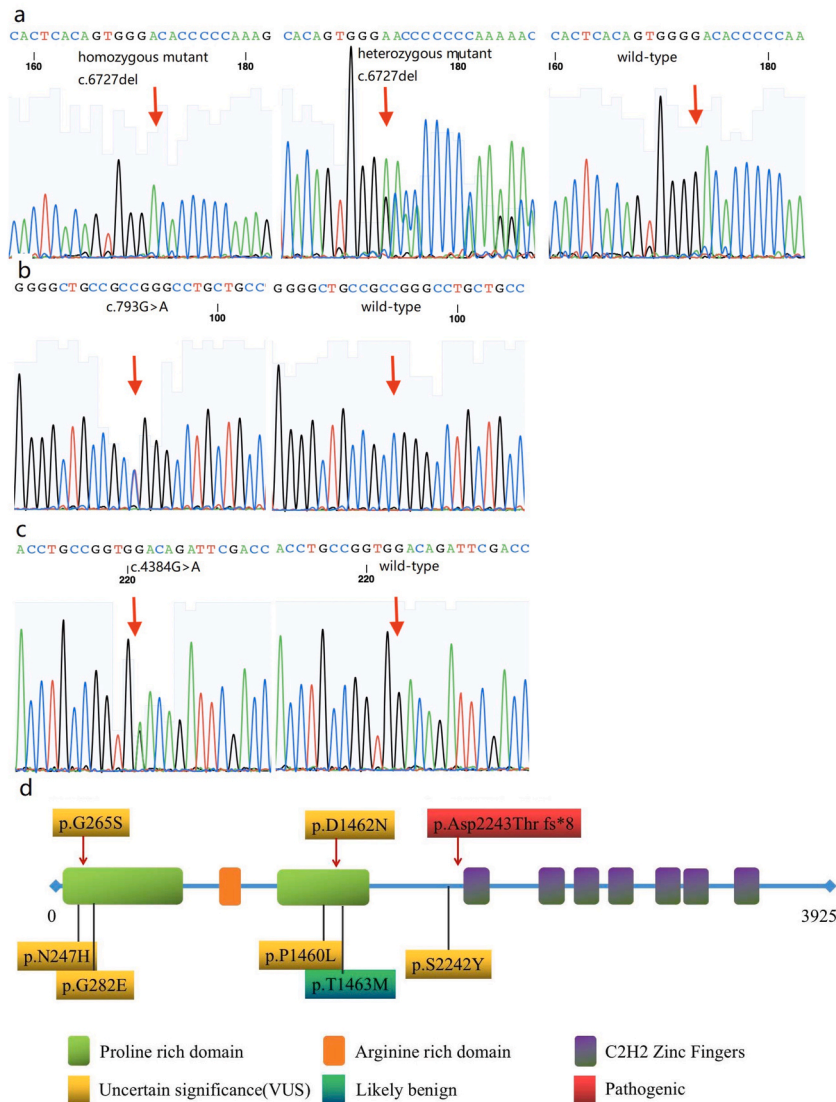


Fig. 5. Identification of new variants in the *ZNF469* gene. **a:** A novel homozygous frameshift mutation c. 6727del (p.Asp2243Thr fs*8) in the proband of the BCS1 family; III:1 and III:2 carried a heterozygous frameshift mutation, IV:2 and III:3 were wild-type; **b:** A heterozygous missense variant g.88494671G > A (c.793G > A, p.G265S, rs754776767) in KC family 1; **c:** A heterozygous missense variant g.88498262G > A (c.4384G > A, p.D1462 N, rs577890057) in KC family 2; **d:** Schematic of *ZNF469* protein domains and the location of variants.

Table 2

Baseline characteristics of the study subjects.

Group	Total, n	Male, n (%)	Female, n (%)	Mean age, years
Patients	368	181 (49.18%)	187 (50.82%)	21.39 ± 6.12
Controls	325	156 (48%)	169 (52%)	20.85 ± 5.52

t-test , $P = 0.1$, χ^2 test, $P = 0.15$.

this mutation is a null variant in a gene where loss-of-function is very strong evidence of pathogenicity (PVS1). In addition, its frequency in the gnomAD population databases is extremely low (PM2) and the phenotype is highly specific for disease, which is supporting-level evidence for pathogenicity (PP4). As a result of this truncation mutation, all seven zinc finger domains are lost, which would lead to protein dysfunction. Previous studies have shown that homozygous *Zfp469* loss-of-function mutation causes BCS in a mouse model [13]. From these findings, c. 6727del (p.Asp2243Thr fs*8) should be considered as pathogenic.

We also examined two Chinese families with KC. Two known single nucleotide polymorphisms were detected (rs754776767 in KC family 1 and rs577890057 in KC family 2). According to the ACMG guidelines, rs754776767 is likely to be a VUS, and the frequency in

Table 3

Distribution of the genotype and allele frequencies of rs754776767 in the patient and control groups.

Group	Genotype			Allele	
	G/G	G/A	A/A	G	A
Patients	356 (96.8)	12 (3.2)	0 (0)	724 (98.7)	12 (1.6)
Controls	325 (100)	0 (0)	0 (0)	650 (100)	0 (0)
p value	0.001			0.001	

Data are shown as n (%).

 χ^2 test.**Table 4**

Distribution of the genotype and allele frequencies of rs577890057 in the patient and control groups.

Group	Genotype			Allele	
	G/G	G/A	A/A	G	A
Patients	358 (97.3)	10 (2.7)	0 (0)	726 (98.64)	10 (1.36)
Controls	325 (100)	0 (0)	0 (0)	650 (100)	0 (0)
p value	0.003			0.003	

Data are shown as n (%).

 χ^2 test.**Table 5**

Distribution of the genotype and allele frequencies of c. 6727del (p.Asp2243Thr fs*8) in the patient and control groups.

Group	Genotype			Allele	
	G/G	G/-	-/-	G	-
Patients	362 (98.4)	6 (1.6)	0 (0)	730 (99.2)	6 (0.8)
Controls	325 (100)	0 (0)	0 (0)	650 (100)	0 (0)
p value	0.02			0.02	

Data are shown as n (%).

 χ^2 test.

the gnomAD population databases is extremely low (PM2). The phenotype is highly specific for disease, providing supporting-level evidence for pathogenicity (PP4). rs577890057 is also likely to be a VUS; the frequency in the gnomAD population databases is extremely low (PM2). The phenotype is highly specific for disease, which is supporting-level evidence for pathogenicity (PP4). We also used computational toolkits (GERP++) to predict the conservation of the variant and used algorithms (Panther classification system) to investigate the effects of the variant on protein structure and function; these analyses revealed the conservation of this variant as GERP++ score = 3.83 [14]. The Leiden Open Variation Database (LOVD) also showed several adjacent sites in *ZNF469* (https://databases.lovd.nl/shared/variants/ZNF469/unique#object_id=VariantOnTranscriptUnique%2CVariantOnGenome&id=ZNF469&search_transcriptid=00023459&page_size=100&page=2) (Fig. 5d). Therefore, these two SNPs might be associated with KC development in the current patients. Notably, the effects of missense variants within proline rich domains (rs754776767 and rs577890057 are within these domains) are still unclear, and many rare missense variants identified within these domains have been reported as VUS for KC [15,16].

We also found that the distribution of the genotype and allele frequencies of *ZNF469* gene was significantly higher in the patient group compared with the control group (All $P < 0.05$. Table 3 for rs754776767, Table 4 for rs577890057, and Table 5 for c. 6727del (p. Asp2243Thr fs*8). Therefore, these three variants may be associated with the susceptibility to keratoconus. Additionally, regarding c. 6727del (p. Asp2243Thr fs*8), III:1 and III:2 (both are heterozygous c. 6727del) in the family with BCS both showed a thinner cornea compared with other family members who do not carry this variant. As a result, we expect that heterozygous c. 6727del may be associated with the susceptibility to keratoconus, while homozygous c. 6727del is associated with BC. Of note, among the patients carrying *ZNF469* variants, none carried two or more *ZNF469* variants. Thus, haplotype association analysis was not conducted.

The 3D structural models of the wild-type protein and the two variants suggest that the mutations cause conformational changes in the *ZNF469* protein. Thus, we have identified allelic enrichment with potential pathogenicity in *ZNF469* of KC patients. Further work is required to determine the functional effects of these variants and the pathways regulated by *ZNF469* that play crucial role in the development of KC. The identification of KC-related pathogenic genes also provide a deeper understanding of the genetic basis of CCT mutations.

The *ZNF469* gene (NM_001127464) is composed of five exons and encodes *ZNF469*, a poorly conserved C2H2 zinc finger (C2H2-ZNF) protein. The *C2H2-ZNF* gene family is the second largest gene family in humans, accounting for 2% of all human genes [17]. The earliest identified members of the C2H2-ZNF family are *Xenopus* TFIIIA and *Drosophila* Kruppel, and therefore the genes of this family are commonly referred to as TFIIIA- or Kruppel-type ZNF genes. Most transcription factors encoded by *C2H2-ZNF* genes bind to DNA,

Table 6

Computational predictions and ACMG classification of all identified variants and their frequency in gnomAD genomes.

Nucleotide change	Amino acid change ^a	rs number	Present in 1 KG data [MAF (%)]	Present in gnomAD_genomes	Present in EVS data [MAF (%)]	SIFT prediction	polyphen2 (score)	Mutation taster	provean
c.793G > A	p.G265S	rs754776767	NO	0.0000647	NO	Tolerated	benign 0.116	Polymorphism	Neutral
c.4384G > A	p.D1462 N	rs577890057	NO	0.00003231	NO	Damaging	Probably damaging 0.991	Polymorphism	Neutral
c. 6727del	p.Asp2243Thr fs*8	N/A	NO	NO	NO	N/A	NA	disease causing	disease causing
Nucleotide change	Amino acid change ^a	rs number	fathmm MKL (score)	grantham _distance	conservarion analysis	ACMG			
c.793G > A	p.G265S	rs754776767	T (0.047)	56	HC	Uncertain significance (PM2_Supporting + PP4)			
c.4384G > A	p.D1462 N	rs577890057	T (0.148)	23	HC	Uncertain significance (PM2_Supporting + PP4)			
c. 6727del	p.Asp2243Thr fs*8	N/A	–	N/A	–	Pathogenic (PVS1+PM2_Supporting + PP4)			

T: tolerated; HC: highly conserved; PM2: absent from controls (or at extremely low frequency if recessive) in Exome Sequencing Project, 1000 Genomes Project, or Exome Aggregation Consortium; PP4: patient's phenotype or family history is highly specific for a disease with a single genetic etiology; PVS1: null variant (nonsense, frameshift, canonical±1 or 2 splice sites, initiation codon, single or multi-exon deletion) in a gene where loss of function is a known mechanism of disease.

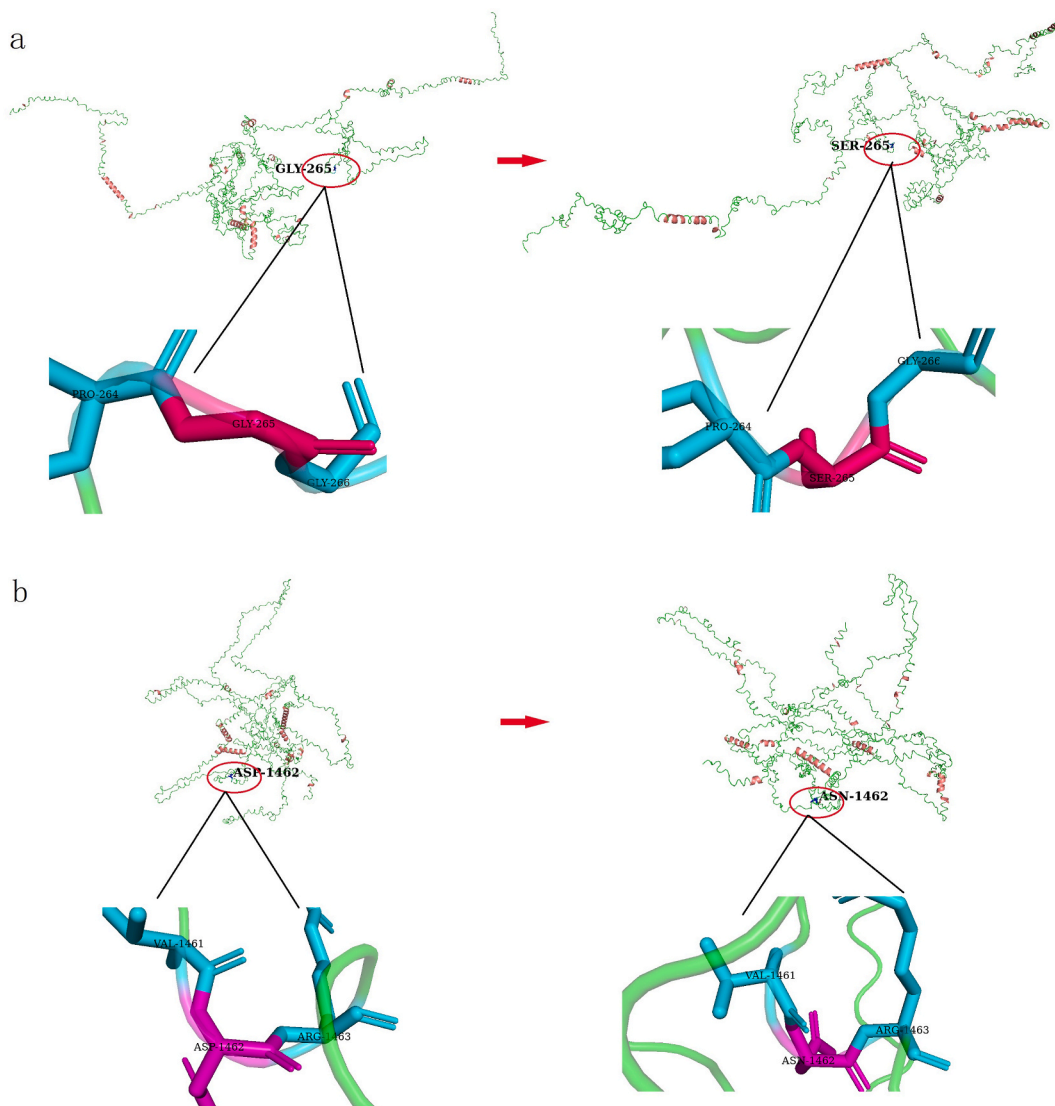


Fig. 6. Three-dimensional structures of the proteins showing the sites of variants. The inset pictures are regional enlargements of the variants. **a:** The three-dimensional structure of wild-type and mutant p.G265S.6b ZNF469; **b:** The three-dimensional structure of wild-type and mutant p.D1462N ZNF469.

RNA, DNA-RNA hybrids and proteins [18,19]. Many genetic studies have demonstrated a role of *ZNF469* in corneal development and suggest that *ZNF469* is a determining factor of corneal thickness. *ZNF469* also functions in regulating the development and maintenance of the extracellular matrix [20].

In humans, the corneal stroma contributes to 90% of the corneal thickness, and resident keratinocytes deposit to form a collagen-rich extracellular matrix. Multiple genes related to the development and maintenance of extracellular matrix were revealed to be downregulated in the genome-wide expression analysis of *ZNF469* mutated fibroblasts, such as EGF-like repeat and discoidin I-like domain-containing protein 3 (*EDIL3*), collagen alpha-1 (IV) chain (*COL4A1*), collagen alpha-1 (XI) chain (*COL11A1*), transforming growth factor beta-2 (*TGFb2*) and hyaluronan and proteoglycan link protein 1 (*HAPLN1*) genes [21]. PPI network analysis also revealed the interaction between *ZNF469* and CCT candidate genes, such as *COL5A1* and *COL1A1*. *ZNF469* also interacts with other genes that regulate eyeball development, such as *VSX1* (causing KC and corneal dystrophy) and *CHST14* (Ehlers-Danlos Syndrome candidate gene); thus, variants in *ZNF469* also could induce abnormal corneal development through disturbing these pathways. *ZNF469* also shows a sequence similarity of 30% with the helical parts of *COL1A1*, *COL1A2* and *COL4A1*, all of which are highly expressed in the cornea [22]. Some evidence has suggested that KC patients may exhibit an imbalance of collagen homeostasis in keratoconus, because 70% of the components in the cornea are collagen, especially type I collagen [23,24].

Recent studies have confirmed that heterozygous *ZNF469* pathological alleles can lead to progressive corneal thinning and dilation, thereby inducing the KC phenotype. Most of the potential pathogenic alleles in KC are missense variants, which may have less harmful

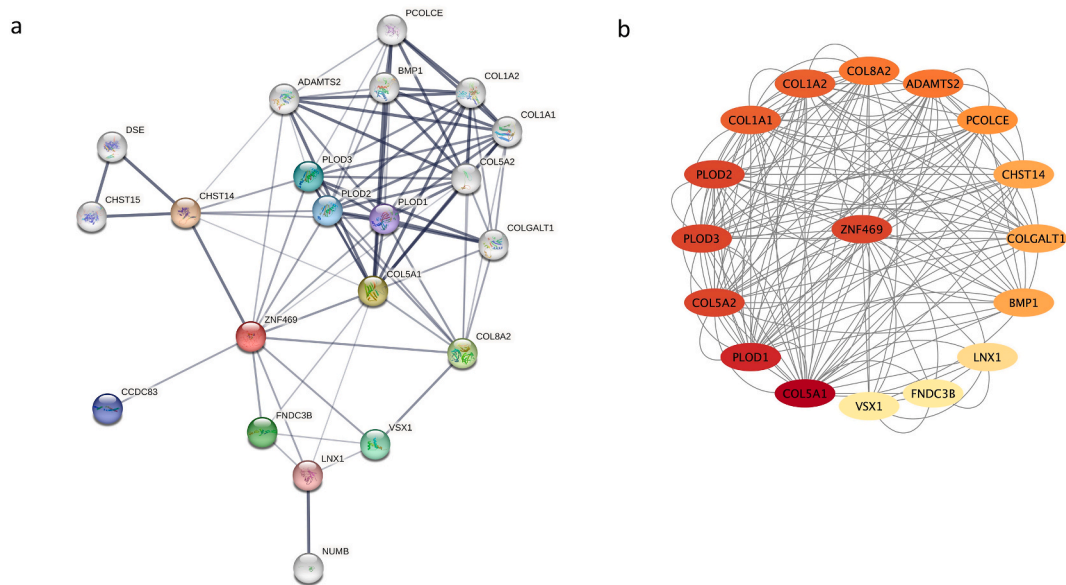


Fig. 7. Topological analysis of the protein-protein interaction network. **a:** The protein-protein interaction network constructed by STRING; **b:** The network of protein-protein interaction performed using Cytoscape.

effects on protein structure and function than the *ZNF469* truncation mutation related to BCS1. This further supports a gene dosage phenomenon, in which homozygous, severely harmful *ZNF469* mutations will lead to an early-onset, severe and visually destructive ocular phenotype, while heterozygous missense *ZNF469* mutations will usually lead to corneal thinning, dilation and KC.

This study has several limitations. This study included one Chinese pedigree with BCS1, two Chinese pedigrees with keratoconus, 368 sporadic keratoconus patients and 325 unrelated healthy controls. The number of pedigrees is limited. More pedigrees and sporadic cases from an Asian population or population with other ethnic background could improve the statistical results and further validate the findings. While the novel frameshift *ZNF469* variant was identified in the BCS1 family, it was considered as pathogenic by silico analysis. Additional animal studies are needed to validate the functionality of this variant. Further investigations are necessary to enhance our understanding of the *ZNF469* variants identified in KC family 1 and KC family 2.

5. Conclusion

Our finding of novel variants in the *ZNF469* gene in three families has widened the spectrum of *ZNF469* variants in BCS and KC. The heterozygous missense mutation of the *ZNF469* pathological allele leads to progressive corneal thinning and dilation, resulting in a KC phenotype. The homozygous frameshift variants may have more harmful effects on protein function, and these truncated mutations are usually associated with BCS1. This further supports a gene dosage phenomenon; with the homozygous, severely harmful *ZNF469* mutation, extreme corneal thinning and dilation may be induced and eventually lead to corneal rupture, while the heterozygous and missense mutation in the *ZNF469* gene is more inclined to lead to KC. Further functional studies and cell-based assays are needed to confirm the molecular pathology and mutation mechanisms associated with these potentially pathogenic *ZNF469* alleles.

Data availability

The datasets generated and analyzed during the current study are available from the corresponding author on reasonable request.

Funding statement

This study received partial funding support from the following projects: the National Natural Science Foundation of China for Young Scholars (No. 82000929); the National Natural Science Foundation of China (No. 81770955); the Shanghai Sailing Program (No. 20YF1405000); the Project of Shanghai Science and Technology (No. 20410710100); the Clinical Research Plan of SHDC (No. SHDC2020CR1043B); the Project of Shanghai Xuhui District Science and Technology (No. 2020-015); the Project of Shanghai Xuhui District Science and Technology (No. XHLHGG202104); the Shanghai Engineering Research Center of Laser and Autostereoscopic 3D for Vision Care (No. 20DZ2255000); and the construction of a 3D digital intelligent prevention and control platform for the whole life cycle of highly myopic patients in the Yangtze River Delta (No. 21002411600).

CRediT authorship contribution statement

Qinghong Lin: Writing – original draft, Supervision, Software, Project administration, Methodology, Formal analysis, Data curation. **Xuejun Wang:** Writing – original draft, Software, Methodology, Formal analysis, Data curation. **Tian Han:** Software, Methodology, Formal analysis, Data curation. **Xiaoliao Peng:** Software, Methodology, Formal analysis, Data curation. **Xingtao Zhou:** Writing – review & editing, Supervision, Project administration, Funding acquisition.

Declaration of competing interest

The authors declare that they have no known competing financial interests or personal relationships that could have appeared to influence the work reported in this paper.

Acknowledgments

The authors would like to express their gratitude to all of the study participants for their cooperation.

Appendix A. Supplementary data

Supplementary data to this article can be found online at <https://doi.org/10.1016/j.heliyon.2024.e27052>.

References

- [1] J. Zlotogora, D. BenEzra, T. Cohen, E. Cohen, Syndrome of brittle cornea, blue sclera, and joint hyperextensibility, *Am. J. Med. Genet.* 36 (1990) 269–272.
- [2] H. Al-Hussain, S.M. Zeisberger, P.R. Huber, C. Giunta, B. Steinmann, Brittle cornea syndrome and its delineation from the kyphoscoliotic type of Ehlers-Danlos syndrome (EDS VI): report on 23 patients and review of the literature, *Am. J. Med. Genet.* 124a (2004) 28–34.
- [3] E.M. Burkitt Wright, L.F. Porter, H.L. Spencer, J. Clayton-Smith, L. Au, F.L. Munier, et al., Brittle cornea syndrome: recognition, molecular diagnosis and management, *Orphanet J. Rare Dis.* 8 (2013) 68.
- [4] T. Dhooge, T. Van Damme, D. Syx, L.M. Mosquera, S. Nampoothiri, A. Radhakrishnan, et al., More than meets the eye: Expanding and reviewing the clinical and mutational spectrum of brittle cornea syndrome, *Hum. Mutat.* 42 (2021) 711–730.
- [5] E.N. Vithana, T. Aung, C.C. Khor, B.K. Cornes, W.T. Tay, X. Sim, et al., Collagen-related genes influence the glaucoma risk factor, central corneal thickness, *Hum. Mol. Genet.* 20 (2011) 649–658.
- [6] Y. Lu, V. Vitart, K.P. Burdon, C.C. Khor, Y. Bykhovskaya, A. Mirshahi, et al., Genome-wide association analyses identify multiple loci associated with central corneal thickness and keratoconus, *Nat. Genet.* 45 (2013) 155–163.
- [7] Y. Bykhovskaya, B. Margines, Y.S. Rabinowitz, Genetics in Keratoconus: where are we? *Eye Vis (Lond)* 3 (2016) 16.
- [8] E. Loukovicis, K. Sfakianakis, P. Syrmakesi, E. Tsotridou, M. Orfanidou, D.R. Bakaloudi, et al., Genetic Aspects of keratoconus: a literature review exploring potential genetic contributions and possible genetic relationships with comorbidities, *Ophthalmol Ther* 7 (2018) 263–292.
- [9] Y. Lu, D.P. Dimasi, P.G. Hysi, A.W. Hewitt, K.P. Burdon, T. Toh, et al., Common genetic variants near the Brittle Cornea Syndrome locus ZNF469 influence the blinding disease risk factor central corneal thickness, *PLoS Genet.* 6 (2010) e1000947.
- [10] R. Hoehn, T. Zeller, V.J. Verhoeven, F. Grus, M. Adler, R.C. Wolfs, et al., Population-based meta-analysis in Caucasians confirms association with COL5A1 and ZNF469 but not COL8A2 with central corneal thickness, *Hum. Genet.* 131 (2012) 1783–1793.
- [11] Q. Lin, L. Zheng, Z. Shen, A novel variant in TGFBI causes keratoconus in a two-generation Chinese family, *Ophthalmic Genet.* 43 (2022) 159–163.
- [12] S. Richards, N. Aziz, S. Bale, D. Bick, S. Das, J. Gastier-Foster, et al., Standards and guidelines for the interpretation of sequence variants: a joint consensus recommendation of the American College of medical genetics and Genomics and the association for molecular pathology, *Genet. Med.* 17 (2015) 405–424.
- [13] C.M. Stanton, A.S. Findlay, C. Drake, M.Z. Mustafa, P. Gautier, L. McKie, et al., A mouse model of brittle cornea syndrome caused by mutation in Zfp469, *Dis Model Mech* (2021) 14.
- [14] [Pantherdb.org](http://www.pantherdb.org/tools/csnpscore.do). Available online: <http://www.pantherdb.org/tools/csnpscore.do> (accessed on 2 December 2022).
- [15] J. Lechner, L.F. Porter, A. Rice, V. Vitart, D.J. Armstrong, D.F. Schorderet, et al., Enrichment of pathogenic alleles in the brittle cornea gene, ZNF469, in keratoconus, *Hum. Mol. Genet.* 23 (2014) 5527–5535.
- [16] A.L. Vincent, C.A. Jordan, M.J. Cadzow, T.R. Merriman, C.N. McGhee, Mutations in the zinc finger protein gene, ZNF469, contribute to the pathogenesis of keratoconus, *Invest. Ophthalmol. Vis. Sci.* 55 (2014) 5629–5635.
- [17] H.D. Tadepally, G. Burger, M. Aubry, Evolution of C2H2-zinc finger genes and subfamilies in mammals: species-specific duplication and loss of clusters, genes and effector domains, *BMC Evol. Biol.* 8 (2008) 176.
- [18] R. Schuh, W. Aicher, U. Gaul, S. Côté, A. Preiss, D. Maier, et al., A conserved family of nuclear proteins containing structural elements of the finger protein encoded by Krüppel, a Drosophila segmentation gene, *Cell* 47 (1986) 1025–1032.
- [19] J.H. Laity, B.M. Lee, P.E. Wright, Zinc finger proteins: new insights into structural and functional diversity, *Curr. Opin. Struct. Biol.* 11 (2001) 39–46.
- [20] M. Rohrbach, H.L. Spencer, L.F. Porter, E.M. Burkitt-Wright, C. Bürer, A. Janecke, et al., ZNF469 frequently mutated in the brittle cornea syndrome (BCS) is a single exon gene possibly regulating the expression of several extracellular matrix components, *Mol. Genet. Metabol.* 109 (2013) 289–295.
- [21] E.M.M. Burkitt Wright, H.L. Spencer, S.B. Daly, F.D.C. Manson, L.A.H. Zeef, J. Urquhart, et al., Mutations in PRDM5 in brittle cornea syndrome identify a pathway regulating extracellular matrix development and maintenance, *Am. J. Hum. Genet.* 88 (2011) 767–777.
- [22] A. Abu, M. Frydman, D. Marek, E. Pras, U. Nir, H. Reznik-Wolf, et al., Deleterious mutations in the Zinc-Finger 469 gene cause brittle cornea syndrome, *Am. J. Hum. Genet.* 82 (2008) 1217–1222.
- [23] J.W. Critchfield, A.J. Calandra, A.B. Nesburn, M.C. Kenney, Keratoconus: I. Biochemical studies, *Exp. Eye Res.* 46 (1988) 953–963.
- [24] M.C. Kenney, A.B. Nesburn, R.E. Burgeson, R.J. Butkowski, A.V. Ljubimov, Abnormalities of the extracellular matrix in keratoconus corneas, *Cornea* 16 (1997) 345–351.